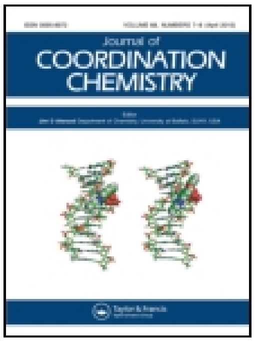

Taylor & Francis
Taylor & Francis Group

Journal of Coordination Chemistry

ISSN: 0095-8972 (Print) 1029-0389 (Online) Journal homepage: http://www.tandfonline.com/loi/gcoo20

2-Benzoimidazol-8-alkylquinolinylnickel(II) complexes as efficient catalysts for ethylene oligomerization and vinyl polymerization of norbornene

Xinfang Wei, Yunqing Jiang, Xue Cui, Yue Li, Haiwang Wang & Xiwei Qi

To cite this article: Xinfang Wei, Yunqing Jiang, Xue Cui, Yue Li, Haiwang Wang & Xiwei Qi (2015) 2-Benzoimidazol-8-alkylquinolinylnickel(II) complexes as efficient catalysts for ethylene oligomerization and vinyl polymerization of norbornene, Journal of Coordination Chemistry, 68:21, 3825-3838, DOI: 10.1080/00958972.2015.1082555

To link to this article: http://dx.doi.org/10.1080/00958972.2015.1082555

Journal of Coordination Chemistry, 2015
Vol. 68, No. 21, 3825–3838, http://dx.doi.org/10.1080/00958972.2015.1082555

2-Benzoimidazol-8-alkylquinolinylnickel(II) complexes as efficient catalysts for ethylene oligomerization and vinyl polymerization of norbornene

XINFANG WEI*†§, YUNQING JIANG§, XUE CUI§, YUE LI§, HAIWANG WANG†‡§ and XIWEI QI*†§

†School of Materials and Metallurgy, Northeastern University, Shenyang, PR China
‡State Key Laboratory of Metastable Materials Science and Technology, Yanshan University, Qinhuangdao, PR China
§Hebei Provincal Laboratory for Dielectric and Electrolyte Materials, Northeastern University at Qinhuangdao, Qinhuangdao, PR China

(*Received 24 March 2015; accepted 30 July 2015*)

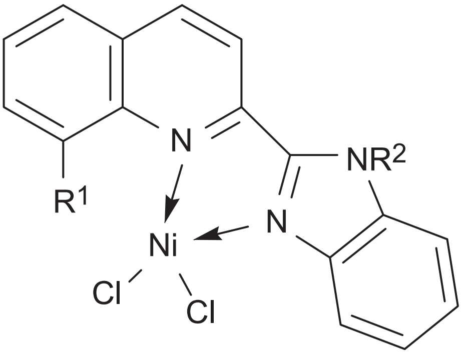

A series of nickel complexes **L**NiCl$_2$ (**C1**–**C16**), where **L** represents 2-benzoimidazol-8-alkylquinoline and its derivatives, were prepared as potential catalysts for the oligomerization of ethylene. The molecular structure of a representative complex **C2**·CH$_3$CH$_2$OH was determined by single-crystal X-ray diffraction. Upon treatment with diethylaluminium chloride (Et$_2$AlCl), all nickel complex pre-catalysts exhibited good activities in the oligomerization of ethylene. Furthermore, in the presence of methylaluminoxane (MAO), the nickel pre-catalysts were suitable for vinyl polymerization of norbornene.

Keywords: Nickel complex; 2-Benzoimidazol-8-alkylquinoline; Ethylene oligomerization; Norbornene polymerization

1. Introduction

With the increasing demand for α-olefins in synthetic lubricants, plasticizers, and surfactants [1], catalysts for the oligomerization of ethylene have gained significant attention in

---

*Corresponding authors. Email: 63525354@qq.com (X. Wei); qxw@mail.neuq.edu.cn (X. Qi) academia and industry [2]. The emergence of the Shell Higher Olefin Process [1,3,4] and highly active pre-catalysts, and the commercialization of dimine-type nickel dichloride complexes [5] revived the research on nickel systems for ethylene polymerization. Accordingly, various nickel complexes have been explored and different ligand sets have been employed, N^N [6–19], N^O [20–25], N^P [26–29], P^O [30,31], P^P [32,33], or tridentate ligands such as N^N^N [34–41], N^N^O [42,43], N^N^P [44,45], and N^P^N [46,47]. In addition, nickel complex pre-catalysts have shown considerable activity in vinyl polymerization of norbornene [48–57] to produce soluble polynorbornenes. *N*,*N*-bidentate Ni(II) complexes have attracted particular attention. Recently, substituted 8-(benzoimidazol-2-yl) quinoline derivatives were employed, and the resulting systems were found to have high activity in the polymerization of ethylene at 100 °C [58,59].

To develop new nickel complex pre-catalysts with high activities, in this study 2-benzoimidazol-8-alkylquinoline derivatives were synthesized and reacted with $NiCl_2$ to obtain nickel complexes. Upon activation with ethylaluminium sesquichloride ($Et_3Al_2Cl_3$, EASC), these nickel complexes exhibited higher activities in the dimerization of ethylene. Moreover, they showed suitable activities in vinyl polymerization of norbornene in the presence of methylaluminoxane (MAO). The catalytic performance of the pre-catalysts in the oligomerization of ethylene and vinyl polymerization of norbornene was investigated.

2. Results and discussion

2.1. *Synthesis and characterization of complexes*

A series of 2-(benzoimidazol-8-yl)quinolines (**L1**–**L16**) were prepared according to scheme 1. All ligands were characterized by FT-IR, ^1H, and ^{13}C NMR spectroscopic measurements, in addition to elemental analysis. Reaction of 2-(benzoimidazol-8-yl) quinolines with an equivalent nickel halide [$NiCl_2 \cdot 6H_2O$] in CH_2Cl_2 afforded the title nickel complexes (scheme 1: **C1**–**C16**) in high yields. All nickel complexes were characterized by FT-IR and elemental analysis, and were highly stable in the solid state and in solution.

In comparison with the FT-IR spectra of the free organic compounds, the absorption bands of the complexes shifted to lower frequencies, suggesting coordination effects. The molecular structure of **C2** was confirmed by single-crystal X-ray diffraction studies.

2.2. *Structural features*

Single crystals of **C2**·CH_3CH_2OH, suitable for X-ray diffraction, were obtained by slow diffusion of diethyl ether into ethanol and DMF solutions. The molecular structure is shown in figure 1, and selected bond lengths and angles are shown in table 1.

In **C2**·CH_3CH_2OH, the geometry around nickel can be described as distorted trigonal bipyramidal, in which the nickel is surrounded by one bidentate ligand, two chlorides, and one CH_3CH_2OH coordinated via oxygen. The axial positions are occupied by N1 of the chelate and O1 of CH_3CH_2OH (O(1)–Ni(1)–N(1) 172.72(12)°), while the equatorial plane is formed by N2 and two chlorides. The Ni1–N2 bond (2.007(3) Å) is significantly shorter than the Ni1–N1 bond (2.103(3) Å), owing to the coordination of the CH_3CH_2OH molecule. Notably, the quinoline ring and benzoimidazole are not coplanar, as they have a dihedral angle of 84.85°.

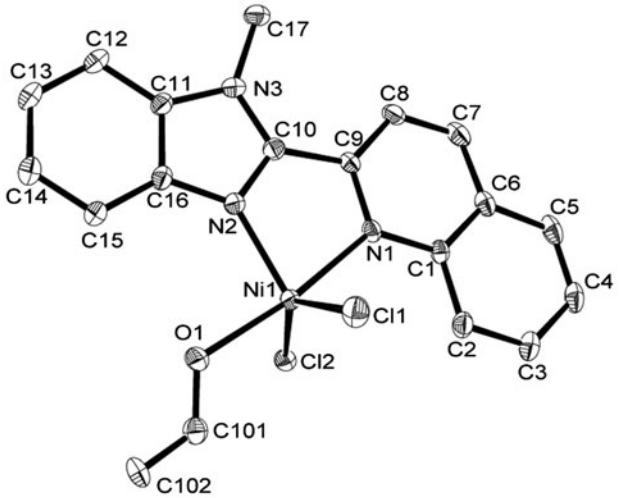

Figure 1. Molecular structure of **C2**·CH_3CH_2OH with thermal ellipsoids at the 30% probability level. Hydrogens have been omitted for clarity.

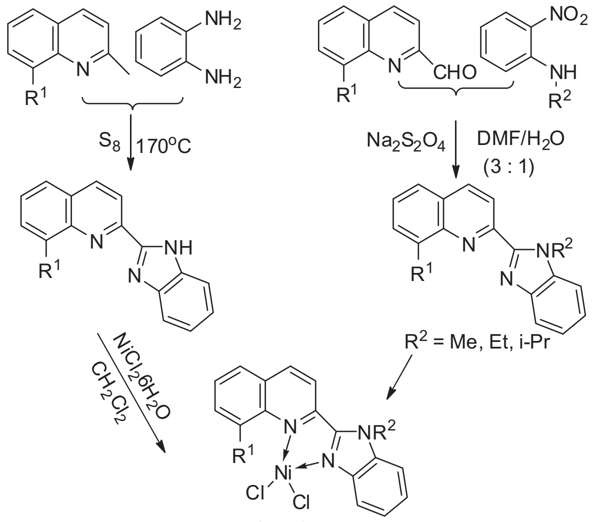

C1 - C16

	L1	**L2**	**L3**	**L4**	**L5**	**L6**	**L7**	**L8**	**L9**	**L10**	**L11**	**L12**	**L13**	**L14**	**L15**	**L16**
	C1	**C2**	**C3**	**C4**	**C5**	**C6**	**C7**	**C8**	**C9**	**C10**	**C11**	**C12**	**C13**	**C14**	**C15**	**C16**
R^1	H	H	H	H	Me	Me	Me	Me	Et	Et	Et	Et	iPr	iPr	iPr	iPr
R^2	H	Me	Et	iPr	H	Me	Et	iPr	H	Me	Et	iPr	H	Me	Et	iPr

Scheme 1. Synthetic procedure.

Table 1. Selected bond lengths (Å) and angles (°) for **C2**·CH_3CH_2OH.

Bond lengths (Å)		Bond angles (°)	
Ni(1)–N(1)	2.103(3)	N(2)–Ni(1)–O(1)	93.91(13)
Ni(1)–N(2)	2.007(3)	N(2)–Ni(1)–N(1)	78.81(13)
Ni(1)–O(1)	2.070(3)	O(1)–Ni(1)–N(1)	172.72(12)
Ni(1)–Cl(1)	2.2945(14)	N(2)–Ni(1)–Cl(1)	112.79(11)
Ni(1)–Cl(2)	2.3126(13)	O(1)–Ni(1)–Cl(1)	91.13(10)
N(1)–C(9)	1.342(5)	N(1)–Ni(1)–Cl(1)	91.61(10)
N(1)–C(1)	1.369(5)	N(2)–Ni(1)–Cl(2)	109.53(11)
N(2)–C(10)	1.317(5)	O(1)–Ni(1)–Cl(2)	92.15(10)
N(2)–C(16)	1.392(5)	N(1)–Ni(1)–Br(2)	90.42(10)
O(1)–C(101)	1.251(5)	Cl(1)–Ni(1)–Cl(2)	137.19(5)

2.3. *Ethylene oligomerization*

2.3.1. Effects of co-catalyst on catalytic behavior. Different co-catalysts, such as methylaluminoxane (MAO), modified methylaluminoxane (MMAO), diethylaluminium chloride (Et_2AlCl), and ethylaluminium sesquichloride ($Et_3Al_2Cl_3$, EASC), were selected as activators of the nickel complexes in the oligomerization of ethylene. The results are presented in table 2. Higher activities were obtained with Et_2AlCl, and the selectivity for C_4 was more than 90%. Notably, **C6** showed activities of up to 3.12×10^6 g mol^{-1}(Ni) h^{-1} upon activation with Et_2AlCl. Therefore, Et_2AlCl was selected for further investigation. In order to determine the optimum results, detailed investigations of **C6** were conducted under various conditions including different molar ratios of the co-catalysts to nickel complex and reaction temperatures under 10 atm of ethylene (table 2).

2.3.2. Effects of reaction parameters on catalytic behavior. As shown in table 3, the reaction parameters had an influence on the catalytic activity in the oligomerization of ethylene. In the **C6**/Et_2AlCl system, the molar ratio of Et_2AlCl to the nickel pro-catalyst (Al/Ni) greatly affected the catalytic activity (entries 4–9, table 2). The optimum Al/Ni molar ratio

Table 2. Ethylene oligomerization with pre-catalyst **C6**.[a]

					Oligomer distribution[c] (%)		
Entry	Co-Cat.	T (°C)	Al/Ni	Activity[b]	α–C_4	C4	C6
1	MAO	30	1000	0.23	88.0	94.0	6.0
2	MMAO	30	1000	0.13	84.0	94.1	5.9
3	EASC	30	200	1.61	80.1	93.7	6.3
4	Et_2AlCl	30	200	2.91	79.3	93.2	6.8
5	Et_2AlCl	30	100	1.45	84.2	93.5	6.5
6	Et_2AlCl	30	250	3.12	78.2	93.9	6.1
7	Et_2AlCl	30	300	2.89	77.6	93.1	6.9
8	Et_2AlCl	30	400	2.47	78.8	93.5	6.5
9	Et_2AlCl	30	500	2.08	77.7	93.4	6.6
10	Et_2AlCl	40	250	2.10	76.5	93.5	6.5
11	Et_2AlCl	50	250	1.18	75.5	93.8	6.2

[a] Conditions: 5 μmol Ni, 10 atm C_2H_4, 20 min, 100 mL of toluene.

[b] Activity, mol^{-1}(Ni) h^{-1}.

[c] Determined by GC, ∑C denotes the total amount of oligomers.

at 30 °C was 250 : 1. The selectivity toward α-olefins and distribution of oligomers varied only slightly. Upon changing the Al/Ni molar ratio, the selectivity toward α-olefins and the distribution of oligomers varied only slightly. However, increasing the reaction temperature resulted in a considerable reduction in catalytic activity (entries 6, 10, and 11 in table 2), potentially because of instability of the active species, or a lower concentration of ethylene in the reaction solution [27,39]. Upon increasing the temperature to 50 °C, much lower activity was observed, in addition to a lower selectivity toward α-olefins. Catalytic activity of 3.12×10^6 g mol^{-1} h^{-1} was observed under the optimized reaction conditions of an Et_2AlCl/Ni molar ratio of 250 : 1, 30 °C reaction temperature, and 10 atm ethylene in the **C6**/Et_2AlCl system.

2.3.3. Effect of ligand substituents on catalytic behavior. To compare the influence of the ligand on the catalytic behavior of the nickel pre-catalysts, chloride pre-catalysts **C1**–**C16** were investigated under the optimized reaction conditions Et_2AlCl/Ni molar ratio of 250 : 1, 30 °C, and 10 atm ethylene, and the data are presented in table 3. The substituents on the quinoline (R^1) and benzoimidazole (R^2) moieties of the ligand affected the catalytic behavior of the nickel complexes and the oligomer distribution. In the series of pre-catalysts with R^1 = Me (entries 4–8, table 3), with the exception of **C5** with R^2 = H, the activity order **C6** (R^2 = Me) > **C7** (R^2 = Et) > **C8** (R^2 = ^{i}Pr) seemed to be governed by the steric hindrance of the ligands and the electron-donating features of the alkyl substituents. Specifically, bulky substituents occupying the space around nickel hinder the coordination of ethylene. This is contradictory to the slow insertion of ethylene on electron-rich active species in catalytic systems with late-transition metals [16,58,59]. The same trend of catalytic activities was observed in the series of nickel pre-catalysts with R^1 = H, Et, or i-Pr, respectively. Therefore, the electronic effect was a major issue caused by the substituent R^2 because R^2 is too far removed from the active nickel center.

Table 3. Ethylene oligomerization by **C1**–**C16**.[a]

			Oligomer distribution[c] (%)		
Entry	Cat.	Activity[b]	α–C_4	C4	C6
1	**C1**	1.88	88.2	93.2	6.8
2	**C2**	1.96	84.1	94.0	6.0
3	**C3**	1.63	82.1	93.1	6.9
4	**C4**	1.55	79.2	93.2	6.8
5	**C5**	2.22	84.2	93.5	6.5
6	**C6**	3.12	78.2	93.9	6.1
7	**C7**	1.88	77.6	93.1	6.9
8	**C8**	1.59	78.8	93.5	6.5
9	**C9**	2.89	77.7	93.4	6.6
10	**C10**	3.13	76.5	93.5	6.5
11	**C11**	2.00	75.5	93.8	6.2
12	**C12**	1.67	88.0	94.0	6.0
13	**C13**	2.99	84.0	94.1	5.9
14	**C14**	3.25	80.1	93.7	6.3
15	**C15**	2.34	79.3	93.2	6.8
16	**C16**	1.77	84.2	93.5	6.5

[a] Conditions: 5 µmol Ni, 250 equiv. Et_2AlCl, 10 atm C_2H_4, 20 min, 100 mL of toluene.
[b] Activity, mol^{-1}(Ni) h^{-1}.
[c] Determined by GC, ∑C denotes the total amount of oligomers.

Table 4. Nobornene polymerization with **C1**–**C12**/MAO.[a]

Run	Cat.	Yield (g)	Activity[b]	Conversion (%)
1	**C1**	2.55	3.06	52.0
2	**C2**	2.77	3.32	56.5
3	**C3**	2.18	2.62	44.6
4	**C4**	2.40	2.87	48.9
5	**C5**	2.42	2.90	49.4
6	**C6**	2.32	2.79	47.5
7	**C7**	1.64	1.96	33.5
8	**C8**	2.51	3.01	51.2
9	**C9**	2.98	3.58	60.8
10	**C10**	3.09	3.71	63.0
11	**C11**	2.40	2.87	48.9
12	**C12**	3.21	3.85	65.5
13	**C13**	1.98	2.39	40.6
14	**C14**	1.79	2.15	36.5
15	**C15**	2.03	2.43	41.4
16	**C16**	2.22	2.66	45.3

[a] Conditions: 2.5 μmol Ni, MAO, Al : Ni : NB = 1000 : 1 : 20,000, total volume 30 mL, 20 °C, 20 min, toluene as solvent.
[b] $\text{mol}^{-1}(\text{Ni})\ \text{h}^{-1}$.

With regard to the influence of the R^1 substituents on the catalytic performances of the nickel complexes, shown with the series of nickel complexes with R^2 = Me, the catalytic activities were in the following order: R^1 = iPr (**C14**) > Et (**C10**) > Me (**C6**) > H (**C2**). This is consistent with the slow insertion of ethylene on the electron-rich active species in late-transition metal catalytic systems [16,59]. Beyond the electronic influence on explaining the better activities, more bulky substituents could protect the active species as R^1 = iPr (**C14**) > Et (**C10**) > Me (**C6**) > H (**C2**). Other series of nickel pre-catalysts with R^2 = H, Et, or i-Pr also exhibited the same trend in their catalytic activities. In general, the main products were butenes with good selectivity toward α-butene reaching 88%.

2.4. *Vinyl polymerization of norbornene*

Although specific applications of polynorbornene remain scarce, there is interest in the use of nickel pre-catalysts in the polymerization of norbornene [54–56]. Thus, the catalytic behaviors of **C1**–**C16** were investigated in the polymerization of norbornene (NB) using toluene as the solvent, and the results are shown in table 4. Upon fixing the Al : Ni : NB molar ratio to 1000/1/20,000, all nickel pre-catalysts showed higher activities at 20 °C, with **C12** exhibiting an activity of 3.85×10^6 g $\text{mol}^{-1}(\text{Ni})\ \text{h}^{-1}$ and a conversion of 65.5%.

3. Conclusion

The preparation of catalyst is very important in the polymerization of organic monomers [60]. R^1 and R^2 showed different influences on the activities of the nickel complexes; therefore, fine-tuning the ligands would potentially control the catalytic activities of nickel pre-catalysts and resultant oligomers, and polymer of norbornene. The $LNiCl_2$ complexes displayed good catalytic activities in the oligomerization of ethylene, and the substituents and reaction parameters affect the catalytic behavior. Activities as high as 3.25×10^6 g (mol Ni)$^{-1}$ h^{-1} were attained using a Al/Ni molar ratio of 250 at 30 °C under 10 bar ethylene. Furthermore, the nickel complexes displayed high activities in the vinyl polymerization of norbornene upon activation with MAO.

4. Experimental

4.1. *General considerations*

All manipulations involving air and moisture-sensitive compounds were carried out under an atmosphere of dried and purified nitrogen using standard Schlenk and vacuum-line techniques. Toluene was dried over sodium metal and distilled under nitrogen. Methylaluminoxane (MAO, 1.46 M solution in toluene) and modified methylaluminoxane (MMAO, 1.93 M in heptane) were purchased from Akzo Nobel Corp. Diethylaluminium chloride (Et_2AlCl, 1.70 M in toluene), triethylaluminium ($AlEt_3$, 2.00 M in heptane), ethylaluminium sesquichloride ($Et_3Al_2Cl_3$, 0.87 M in toluene), and other reagents were purchased from Acros Chemicals. FT-IR spectra were recorded on a Perkin–Elmer System 2000 FT-IR spectrometer. Elemental analysis was carried out using a Flash EA 1112 microanalyzer. GC analyses were performed using a Varian CP-3800 gas chromatograph equipped with a flame ionization detector and a 30 m (0.2 mm i.d., 0.25-μm film thickness) CP-Sil 5 CB column.

4.2. *Syntheses and characterizations*

L1 A mixture of 2-methylquinoline (1.43 g, 10 mmol), benzene-1,2-diamine (1.08 g, 10 mmol), and PPA (1.43 g, 10 mmol) was refluxed for 12 h at 170 °C. The eluted fraction was collected and concentrated to give **L1** as a yellow solid in a 43% yield. δ_H (400 MHz; $CDCl_3$; Me_4Si) 10.96 (1H, s), 8.56 (1H, d, $J = 8.1$ Hz), 8.32 (1H, d, $J = 8.6$ Hz), 8.11 (1H, d, $J = 8.5$ Hz), 7.89 (2H, t, $J = 11.3$ Hz), 7.75 (1H, t, $J = 10.2$ Hz), 7.58 (1H, t, $J = 10.0$ Hz), 7.49 (1H, d, $J = 7.8$ Hz), 7.29–7.33 (2H, m), 4.46 (3H, s, $-CH_3$). δ_C (100 MHz; $CDCl_3$; Me_4Si) 151.1, 148.5, 147.6, 144.6, 137.5, 134.2, 130.4, 129.0, 128.7, 128.0, 127.4, 124.3, 122.8, 120.4, 119.4, 111.4. Anal. Calcd for $C_{16}H_{11}N_3$ (245.28): C, 78.35; H, 4.52; N, 17.13. Found: C, 78.25; H, 4.72; N, 17.00. FT-IR (diamond disk, cm^{-1}): 3047, 1652, 1597, 1496, 1444, 1414, 1317, 1233, 1105, 867, 829, 737.

L2 A mixture of quinoline-2-carbaldehyde (1.57 g, 10.0 mmol), N-methyl-2-nitrobenzenamine (1.52 g, 10.0 mmol), $Na_2S_2O_4$ (3.20 g), and DMF : H_2O (3 : 1) was refluxed for 12 h. The solvent was evaporated on a rotary evaporator and the resulting solid was eluted with petroleum ether on an alumina column. The second fraction was collected and concentrated to give **L2** as a yellow solid in 46% yield. δ_H (400 MHz; $CDCl_3$; Me_4Si) 8.55 (1H, d, $J = 8.6$ Hz), 8.28 (1H, d, $J = 8.6$ Hz), 8.16 (1H, d, $J = 8.6$ Hz), 7.87 (2H, t, $J = 10.9$ Hz), 7.76 (1H, t, $J = 10.1$ Hz), 7.59 (1H, t, $J = 10.1$ Hz), 7.48 (1H, d, $J = 7.8$ Hz), 7.35 (2H, m), 4.46 (3H, s, $-CH_3$). δ_C (100 MHz; $CDCl_3$; Me_4Si) 150.4, 149.8, 147.1, 142.6, 137.5, 136.3, 129.6, 129.5, 127.6, 127.5, 127.1, 123.5, 122.6, 121.6, 120.2, 110.0, 32.99. Anal. Calcd for $C_{17}H_{13}N_3$ (259.31): C, 78.74; H, 5.05; N, 16.20. Found: C, 78.64; H, 5.15; N, 16.10. FT-IR (diamond disk, cm^{-1}): 3047, 1616, 1598, 1466, 1446, 1390, 1332, 1211, 1115, 1053, 1008, 838, 764, 734.

L3 In a manner similar to that described for **L2**, **L3** was prepared as a yellow solid in 36% yield. δ_H (400 MHz; $CDCl_3$; Me_4Si) 8.57 (1H, d, J = 8.6 Hz), 8.28 (1H, d, J = 8.6 Hz), 8.14 (1H, d, J = 8.4 Hz), 7.88 (2H, m), 7.76 (1H, t, J = 10.1 Hz), 7.59 (1H, t, J = 10.1 Hz), 7.48 (1H, d, J = 7.8 Hz), 7.37 (1H, t, J = 9.3 Hz), 7.33 (1H, t, J = 9.2 Hz), 5.02–5.07 (2H, m, $–CH_2–$), 1.64 (3H, t, J = 9.5 Hz, $–CH_3$). δ_C (100 MHz; $CDCl_3$; Me_4Si) 150.4, 149.6, 147.4, 142.9, 136.6, 136.4, 129.7, 127.7, 127.2, 123.6, 122.7, 121.8, 120.4, 110.1, 40.96, 15.47. Anal. Calcd for $C_{18}H_{15}N_3$ (273.33): C, 79.10; H, 5.53; N, 15.37. Found: C, 78.64; H, 5.15; N, 16.10. FT-IR (diamond disk, cm^{-1}): 3046, 1598, 1560, 1467, 1396, 1329, 1257, 1189, 1117, 1067, 827, 758, 734.

L4 In a manner similar to that described for **L2**, **L4** was prepared as a yellow solid in 29% yield. δ_H (400 MHz; $CDCl_3$; Me_4Si) 8.43 (1H, d, J = 8.6 Hz), 8.30 (1H, d, J = 8.6 Hz), 8.14 (1H, d, J = 8.4 Hz), 7.89 (2H, m), 7.71–7.78 (2H, m), 7.60 (1H, t, J = 7.8 Hz), 7.32 (1H, t, J = 9.3 Hz), 7.30 (1H, t, J = 9.2 Hz), 5.02–5.07 (2H, m, $–CH_2–$), 1.64 (3H, t, J = 9.5 Hz, $–CH_3$). δ_C (100 MHz; $CDCl_3$; Me_4Si) 150.9, 150.4, 147.2, 143.6, 136.6, 134.9, 129.9, 129.8, 127.8, 127.7, 127.3, 123.0, 122.6, 122.3, 120.7, 113.1, 49.12, 21.44. Anal. Calcd for $C_{19}H_{17}N_3$ (287.36): C, 79.41; H, 5.96; N, 14.62. Found: C, 78.64; H, 5.15; N, 16.10. FT-IR (diamond disk, cm^{-1}): 2969, 1596, 1494, 1390, 1255, 1114, 833, 765, 742.

L5 In a manner similar to that described for **L1**, **L5** was prepared as a yellow solid in 47% yield. δ_H (400 MHz; $CDCl_3$; Me_4Si) 10.65 (1H, s), 8.52 (1H, d, J = 8.6 Hz), 8.27 (1H, d, J = 8.6 Hz), 7.89 (1H, d, J = 8.4 Hz), 7.76 (1H, t, J = 9.9 Hz), 7.59 (1H, t, J = 10.0 Hz), 7.46 (1H, t, J = 9.8 Hz), 7.32 (2H, m), 2.87 (3H, s, $–CH_3$). δ_C (100 MHz; $CDCl_3$; Me_4Si) 151.4, 151.0, 146.6, 145.0, 137.5, 137.2, 136.6, 130.3, 128.6, 127.1, 125.9, 124.4, 120.3, 119.7, 118.7, 111.4, 18.08. Anal. Calcd for $C_{17}H_{13}N_3$ (259.31): C, 78.74; H, 5.05; N, 16.20. Found: C, 78.64; H, 5.15; N, 16.10. FT-IR (diamond disk, cm^{-1}): 2921, 1596, 1491, 1413, 1314, 837, 736.

L6 In a manner similar to that described for **L2**, **L6** was prepared as a yellow solid in 43% yield. δ_H (400 MHz; $CDCl_3$; Me_4Si) 8.60 (1H, d, J = 8.6 Hz), 8.24 (1H, d, J = 8.6 Hz), 7.90 (1H, d, J = 8.4 Hz), 7.66 (1H, d, J = 8.0 Hz), 7.54 (1H, d, J = 7.0 Hz), 7.46 (2H, m), 7.34 (2H, t, J = 7.3 Hz), 4.50 (3H, s, $–CH_3$), 2.87 (3H, s, $–CH_3$). δ_C (100 MHz; $CDCl_3$; Me_4Si) 150.3, 149.3, 146.4, 142.7, 137.5, 136.8, 129.9, 127.7, 127.0, 125.7, 123.6, 122.6, 121.4, 120.2, 110.0, 33.39, 18.48. Anal. Calcd for $C_{18}H_{15}N_3$ (273.33): C, 79.10; H, 5.53; N, 15.37. Found: C, 78.64; H, 5.15; N, 16.10. FT-IR (diamond disk, cm^{-1}): 2915, 1600, 1568, 1490, 1413, 1388, 1330, 1205, 1055, 843, 764, 733.

L7 In a manner similar to that described for **L2**, **L7** was prepared as a yellow solid in 39% yield. δ_H (400 MHz; $CDCl_3$; Me_4Si) 8.59 (1H, d, J = 8.6 Hz), 8.26 (1H, d, J = 8.6 Hz), 7.89 (1H, d, J = 8.6 Hz), 7.71 (1H, d, J = 8.0 Hz), 7.61 (1H, d, J = 7.0 Hz), 7.48 (2H, m), 7.35 (2H, t, J = 7.3 Hz), 5.04–5.07 (2H, m, $–CH_2–$), 2.83 (3H, s, $–CH_3$), 1.59 (3H, m, $–CH_3$). δ_C (100 MHz; $CDCl_3$; Me_4Si) 149.6, 149.3, 146.6, 142.8, 137.5, 136.8, 136.6, 130.0, 127.7, 127.0, 125.7, 123.6, 122.6, 121.6, 120.3, 110.0, 40.92, 18.45, 15.54. Anal. Calcd for $C_{19}H_{17}N_3$ (287.36): C, 79.41; H, 5.96; N, 14.62. Found: C, 78.64; H, 5.15; N, 16.10. FT-IR (diamond disk, cm^{-1}): 2969, 1599, 1571, 1398, 1371, 1325, 1257, 1189, 1127, 1074, 841, 766, 746.

L8 In a manner similar to that described for **L2**, **L8** was prepared as a yellow solid in 18% yield. δ_H (400 MHz; $CDCl_3$; Me_4Si) 8.47 (1H, d, J = 8.6 Hz), 8.29 (1H, d, J = 8.6 Hz), 7.89 (1H, d, J = 8.4 Hz), 7.71 (2H, t, J = 10.0 Hz), 7.59 (1H, d, J = 7.0 Hz), 7.49 (1H, t, J = 9.8 Hz), 7.31 (2H, m), 6.57–6.45 (1H, m, –CH–), 2.82 (3H, s, $–CH_3$), 1.80 (6H, d, J = 7.6, 2×$–CH_3$). δ_C (100 MHz; $CDCl_3$; Me_4Si) 150.5, 149.7, 146.3, 143.6, 137.5, 137.0, 134.9, 130.0, 127.7, 127.2, 125.8, 122.9, 122.4, 122.2, 120.7, 113.1, 49.10, 21.49, 18.26. Anal. Calcd for $C_{20}H_{19}N_3$ (301.38): C, 79.70; H, 6.35; N, 13.94. Found: C, 78.64; H, 5.15; N, 16.10. FT-IR (diamond disk, cm^{-1}): 2956, 1601, 1474, 1435, 1387, 1325, 1211, 1055, 840, 758, 736.

L9 In a manner similar to that described for **L1**, **L9** was prepared as a yellow solid in 43% yield. δ_H (400 MHz; $CDCl_3$; Me_4Si) 10.51 (1H, s), 8.52 (1H, d, *J* = 8.5 Hz), 8.29 (1H, d, *J* = 8.5 Hz), 7.90 (1H, d, *J* = 7.4 Hz), 7.71 (1H, d, *J* = 8.0 Hz), 7.61 (2H, t, *J* = 8.6 Hz), 7.51 (1H, t, *J* = 10.1 Hz), 7.34 (2H, d, *J* = 8.3 Hz), 3.39–3.45 (2H, m, $-CH_2-$), 1.47 (3H, t, *J* = 10.1 Hz, $-CH_3$). δ_C (100 MHz; $CDCl_3$; Me_4Si) 151.6, 146.9, 146.0, 144.7, 142.9, 137.7, 134.1, 128.8, 128.6, 127.3, 125.9, 124.3, 122.8, 120.4, 118.7, 111.4, 24.54, 15.25. Anal. Calcd for $C_{18}H_{15}N_3$ (273.33): C, 79.10; H, 5.53; N, 15.37. Found: C, 78.64; H, 5.15; N, 16.10. FT-IR (diamond disk, cm^{-1}): 2959, 1597, 1495, 1411, 1313, 1227, 842, 740.

L10 In a manner similar to that described for **L2**, **L10** was prepared as a yellow solid in 40% yield. δ_H (400 MHz; $CDCl_3$; Me_4Si) 8.59 (1H, d, *J* = 8.6 Hz), 8.25 (1H, d, *J* = 8.6 Hz), 7.89 (1H, d, *J* = 7.5 Hz), 7.70 (1H, d, *J* = 8.0 Hz), 7.61 (1H, d, *J* = 6.9 Hz), 7.49 (2H, t, *J* = 6.5 Hz), 7.35 (2H, t, *J* = 7.3 Hz), 4.89 (3H, s, $-CH_3$), 3.33–3.39 (2H, m, $-CH_2-$), 1.64 (3H, t, *J* = 9.4 Hz, $-CH_3$), 1.43 (3H, t, *J* = 9.9 Hz, $-CH_3$). δ_C (100 MHz; $CDCl_3$; Me_4Si) 150.1, 149.3, 145.6, 143.1, 142.6, 137.5, 136.8, 128.2, 127.7, 127.1, 125.6, 123.5, 122.6, 121.3, 120.2, 109.9, 33.17, 24.91, 15.02. Anal. Calcd for $C_{19}H_{17}N_3$ (287.36): C, 79.41; H, 5.96; N, 14.62. Found: C, 78.64; H, 5.15; N, 16.10. FT-IR (diamond disk, cm^{-1}): 2924, 1602, 1475, 1438, 1390, 1367, 1321, 1211, 1058, 850, 735.

L11 In a manner similar to that described for **L2**, **L11** was prepared as a yellow solid in 35% yield. δ_H (400 MHz; $CDCl_3$; Me_4Si) 8.62 (1H, d, *J* = 8.6 Hz), 8.27 (1H, d, *J* = 8.2 Hz), 7.89 (1H, d, *J* = 7.3 Hz), 7.72 (1H, d, *J* = 8.0 Hz), 7.62 (1H, d, *J* = 8.6 Hz), 7.54 (2H, t, *J* = 6.5 Hz), 7.35 (2H, t, *J* = 7.3 Hz), 5.10–5.15 (2H, m, $-CH_2-$), 3.28–3.39 (2H, m, $-CH_2-$), 1.64 (3H, t, *J* = 9.4 Hz, $-CH_3$), 1.42 (3H, t, *J* = 9.9 Hz, $-CH_3$). δ_C (100 MHz; $CDCl_3$; Me_4Si) 149.7, 149.4, 145.8, 143.2, 142.9, 136.9, 136.5, 128.4, 127.9, 127.2, 125.7, 123.6, 122.7, 121.7, 120.3, 110.0, 40.79, 24.76, 15.60, 15.41. Anal. Calcd for $C_{20}H_{19}N_3$ (301.38): C, 79.70; H, 6.35; N, 13.94. Found: C, 78.64; H, 5.15; N, 16.10. FT-IR (diamond disk, cm^{-1}): 2927, 1601, 1441, 1396, 1371, 1324, 1188, 1055, 842, 764, 729.

L12 In a manner similar to that described for **L2**, **L12** was prepared as a yellow solid in 28% yield. δ_H (400 MHz; $CDCl_3$; Me_4Si) 8.47 (1H, d, *J* = 8.6 Hz), 8.29 (1H, d, *J* = 8.6 Hz), 7.90 (1H, d, *J* = 8.6 Hz), 7.71 (2H, m), 7.61 (1H, d, *J* = 7.0 Hz), 7.52 (2H, m), 7.32 (2H, t, *J* = 7.3 Hz), 6.64–6.53 (1H, m, –CH–), 3.33 (2H, m, $-CH_2-$), 1.80 (6H, d, *J* = 7.0 Hz, $2\times-CH_3$), 1.41–1.37 (3H, m, $-CH_3$). δ_C (100 MHz; $CDCl_3$; Me_4Si) 150.3, 149.7, 145.5, 143.8, 143.0, 137.1, 135.0, 128.6, 127.8, 127.3, 125.8, 125.7, 123.1, 122.4, 120.8, 113.2, 48.96, 25.07, 24.58, 21.32, 15.58, 15.13. Anal. Calcd for $C_{21}H_{21}N_3$ (315.41): C, 79.97; H, 6.71; N, 13.32. Found: C, 78.64; H, 5.15; N, 16.10. FT-IR (diamond disk, cm^{-1}): 2959, 1598, 1465, 1449, 1399, 1372, 1330, 1175, 854, 763, 734.

L13 In a manner similar to that described for **L1**, **L13** was prepared as a yellow solid in 45% yield. δ_H (400 MHz; $CDCl_3$; Me_4Si) 10.52 (1H, s), 8.52 (1H, d, *J* = 8.3 Hz), 8.30 (1H, d, *J* = 8.0 Hz), 7.90 (1H, d, *J* = 7.0 Hz), 7.71 (1H, d, *J* = 7.4 Hz), 7.67 (1H, d, *J* = 8.5 Hz), 7.62 (1H, d, *J* = 6.5 Hz), 7.56 (1H, t, *J* = 7.3 Hz), 7.34 (2H), 4.48 (1H, m, –CH–), 1.46 (6H, $2\times CH_3$). δ_C (100 MHz; $CDCl_3$; Me_4Si) 151.6, 147.3, 146.8, 145.4, 144.7, 137.8, 134.1, 128.8, 127.4, 126.0, 125.7, 124.3, 122.8, 120.4, 118.6, 111.4, 27.44, 23.71. Anal. Calcd for $C_{19}H_{17}N_3$ (287.36): C, 79.41; H, 5.96; N, 14.62. Found: C, 78.64; H, 5.15; N, 16.10. FT-IR (diamond disk, cm^{-1}): 2955, 1598, 1496, 1413, 1312, 1276, 840, 763, 741.

L14 In a manner similar to that described for **L2**, **L14** was prepared as a yellow solid in 41% yield. δ_H (400 MHz; $CDCl_3$; Me_4Si) 8.59 (1H, d, $J = 8.6$ Hz), 8.27 (1H, d, $J = 8.6$ Hz), 7.90 (1H, d, $J = 7.8$ Hz), 7.71 (1H, d, $J = 8.0$ Hz), 7.67 (1H, d, $J = 7.1$ Hz), 7.56 (1H, t, $J = 10.1$ Hz), 7.49 (1H, d, $J = 7.8$ Hz), 7.39–7.31 (2H, m), 4.40 (1H, m, –CH–), 1.44 (3H, d, $J = 7.2$, 2 × CH_3). δ_C (100 MHz; $CDCl_3$; Me_4Si) 150.5, 149.3, 147.6, 145.2, 142.7, 137.6, 137.2, 127.9, 127.4, 125.7, 125.6, 123.7, 122.7, 121.5, 120.3, 110.0, 33.31, 27.72, 23.56. Anal. Calcd for $C_{20}H_{19}N_3$ (301.38): C, 79.70; H, 6.35; N, 13.94. Found: C, 78.64; H, 5.15; N, 16.10. FT-IR (diamond disk, cm^{-1}): 2952, 1598, 1568, 1481, 1412, 1303, 1280, 1228, 1121, 865, 839, 740.

L15 In a manner similar to that described for **L2**, **L15** was prepared as a yellow solid in 34% yield. δ_H (400 MHz; $CDCl_3$; Me_4Si) 8.61 (1H, d, $J = 8.6$ Hz), 8.27 (1H, d, $J = 8.6$ Hz), 7.88 (1H, d, $J = 7.6$ Hz), 7.70 (1H, d, $J = 8.1$ Hz), 7.67 (1H, d, $J = 7.0$ Hz), 7.58–7.50 (2H, m), 7.38–7.31 (2H, m), 5.15–5.09 (2H, m, –CH_2–), 4.43–4.36 (1H, m, –CH–), 1.62 (3H, t, $J = 9.5$ Hz, –CH_3), 1.43 (6H, d, $J = 7.2$ Hz, 2×–CH_3). δ_C (100 MHz; $CDCl_3$; Me_4Si) 149.9, 149.5, 147.6, 145.4, 142.9, 137.2, 136.6, 128.0, 127.4, 125.7, 123.7, 122.7, 121.8, 120.4, 110.1, 40.84, 27.43, 23.80, 15.71. Anal. Calcd for $C_{21}H_{21}N_3$ (315.41): C, 79.97; H, 6.71; N, 13.32. Found: C, 78.64; H, 5.15; N, 16.10. FT-IR (diamond disk, cm^{-1}): 2991, 1599, 1466, 1415, 1388, 1343, 1180, 1131, 1016, 844, 743.

L16 In a manner similar to that described for **L2**, **L16** was prepared as a yellow solid in 20% yield. δ_H (400 MHz; $CDCl_3$; Me_4Si) 8.47 (1H, d, $J = 8.6$ Hz), 8.29 (1H, d, $J = 8.6$ Hz), 7.89 (1H, d, $J = 7.6$ Hz), 7.74 (2H, m), 7.67 (1H, d, $J = 7.0$ Hz), 7.54 (1H, t, $J = 10.0$), 7.33–7.31 (2H, m), 6.61–6.56 (1H, m, –CH–), 4.38–4.32 (1H, m, –CH–), 1.79 (6H, d, $J = 7.5$ Hz, –CH_3), 1.43 (6H, d, $J = 7.2$ Hz, 2×–CH_3). δ_C (100 MHz; $CDCl_3$; Me_4Si) 150.5, 149.7, 147.5, 145.1, 143.7, 137.3, 134.9, 127.9, 127.4, 125.6, 123.0, 122.4, 122.3, 120.8, 113.7, 49.00, 27.64, 23.62, 22.83, 21.49. Anal. Calcd for $C_{22}H_{23}N_3$ (329.44): C, 80.21; H, 7.04; N, 12.76. Found: C, 78.64; H, 5.15; N, 16.10. FT-IR (diamond disk, cm^{-1}): 2961, 1600, 1456, 1425, 1388, 1333, 1179, 1131, 1015, 844, 737.

C1 In a Schlenk tube with 10 mL of dried ethanol, **L1** (0.245 g, 1.0 mmol) and $NiCl_2·6H_2O$ (0.236 g, 1.0 mmol) were added, and the mixture was stirred for 12 h at room temperature. Absolute diethyl ether (10 mL) was added to precipitate the complex. The precipitate was washed with diethyl ether and dried under vacuum to obtain **C1** as a yellow powder in 83% yield. Calcd for $C_{16}H_{11}Cl_2N_3Ni$ (374.88): C, 51.26; H, 2.96; N, 11.21%. Found: C, 51.16; H, 3.03; N, 11.09%. FT-IR (diamond; cm^{-1}): 3345, 1622, 1596, 1507, 1430, 1319, 1145, 832, 740.

C2 In a manner similar to that described for **C1**, **C2** was prepared as a yellow powder in 86% yield. In comparison with the FT-IR spectra of the free organic compounds, the absorption bands of the complexes were shifted to lower frequencies, suggesting coordination effects. Anal. Calcd for $C_{17}H_{13}Br_2N_3Ni$ (388.90): C, 52.50; H, 3.37; N, 10.80%. Found: C, 52.35; H, 3.43; N, 10.73%. EIMS m/z 440.87$[M]^+$ (23), 234(20), 200(40), 80 (100). FT-IR (diamond; cm^{-1}): 3051, 1591, 1474, 1410, 1348, 1140, 1101, 827, 744.

C3 In a manner similar to that described for **C1**, **C3** was prepared as a yellow powder in 85% yield. Anal. Calcd for $C_{18}H_{15}Cl_2N_3Ni$ (402.93): C, 53.65; H, 3.75; N, 10.43%. Found: C, 53.50; H, 3.85; N, 10.32%. FT-IR (diamond; cm^{-1}): 2976, 1591, 1524, 1500, 1424, 1338, 1141, 827, 758, 740.

C4 In a manner similar to that described for **C1**, **C4** was prepared as a yellow powder in 82% yield. Anal. Calcd for $C_{19}H_{17}Cl_2N_3Ni$ (416.96): C, 54.73; H, 4.11; N, 10.08%. Found: C, 54.58; H, 4.24; N, 10.00%. FT-IR (diamond; cm^{-1}): 3328, 1589, 1463, 1427, 1337, 1162, 832, 747.

C5 In a manner similar to that described for **C1**, **C5** was prepared as a yellow powder in 91% yield. Anal. Calcd for $C_{17}H_{13}Cl_2N_3Ni$ (388.90): C, 52.50; H, 3.37; N, 10.80%. Found: C, 52.40; H, 3.52; N, 10.68%. FT-IR (diamond; cm^{-1}): 3052, 1598, 1478, 1419, 1320, 839, 756.

C6 In a manner similar to that described for **C1**, **C6** was prepared as a yellow powder in 87% yield. Anal. Calcd for $C_{18}H_{15}Cl_2N_3Ni$ (402.93): C, 53.65; H, 3.75; N, 10.43%. Found: C, 53.55; H, 3.87; N, 10.31%. FT-IR (diamond; cm^{-1}): 3336, 1593, 1474, 1400, 1349, 1152, 831, 757.

C7 In a manner similar to that described for **C1**, **C7** was prepared as a yellow powder in 83% yield. Anal. Calcd for $C_{19}H_{17}Cl_2N_3Ni$ (416.96): C, 54.73; H, 4.11; N, 10.08%. Found: C, 54.56; H, 4.29; N, 10.00%. FT-IR (diamond; cm^{-1}): 3351, 1590, 1445, 1348, 1157, 845, 742.

C8 In a manner similar to that described for **C1**, **C8** was prepared as a yellow powder in 82% yield. Anal. Calcd for $C_{20}H_{19}Cl_2N_3Ni$ (430.98): C, 55.74; H, 4.44; N, 9.75%. Found: C, 55.56; H, 4.55; N, 9.65%. FT- IR (diamond; cm^{-1}): 3042, 1594, 1479, 1413, 1320, 840, 752.

C9 In a manner similar to that described for **C1**, **C9** was prepared as a yellow powder in 89% yield. Anal. Calcd for $C_{18}H_{15}Cl_2N_3Ni$ (402.93): C, 53.65; H, 3.75; N, 10.43%. Found: C, 53.55; H, 3.87; N, 10.32%. FT-IR (diamond; cm^{-1}): 3342, 1590, 1533, 1429, 1351, 1163, 857, 734.

C10 In a manner similar to that described for **C1**, **C10** was prepared as a yellow powder in 90% yield. Anal. Calcd for $C_{19}H_{17}Cl_2N_3Ni$ (416.96): C, 54.73; H, 4.11; N, 10.08%. Found: C, 54.56; H, 4.22; N, 10.00%. FT-IR (diamond; cm^{-1}): 3332, 1591, 1531, 1437, 1349, 1163, 846, 744.

C11 In a manner similar to that described for **C1**, **C11** was prepared as a yellow powder in 86% yield. Anal. Calcd for $C_{20}H_{19}Cl_2N_3Ni$ (430.98): C, 55.74; H, 4.44; N, 9.75%. Found: C, 55.62; H, 4.56; N, 9.65%. FT-IR (diamond; cm^{-1}): 3368, 1600, 1567, 1397, 1371, 1188, 1056, 842, 765, 729.

C12 In a manner similar to that described for **C1**, **C12** was prepared as a yellow powder in 83% yield. Anal. Calcd for $C_{21}H_{21}Cl_2N_3Ni$ (445.01): C, 56.68; H, 4.76; N, 9.44%. Found: C, 56.54; H, 4.83; N, 9.34%. FT-IR (diamond; cm^{-1}): 3256, 1594, 1545, 1390, 1345, 1189, 1052, 840, 765, 739.

C13 In a manner similar to that described for **C1**, **C13** was prepared as a yellow powder in 87% yield. Anal. Calcd for $C_{19}H_{17}Cl_2N_3Ni$ (416.96): C, 54.73; H, 4.11; N, 10.08%. Found: C, 54.57; H, 4.24; N, 10.00%. FT-IR (diamond; cm^{-1}): 3325, 1600, 1496, 1412, 1312, 838, 738.

C14 In a manner similar to that described for **C1**, **C14** was prepared as a yellow powder in 91% yield. Anal. Calcd for $C_{20}H_{19}Cl_2N_3Ni$ (430.98): C, 55.74; H, 4.44; N, 9.75%. Found: C, 55.64; H, 4.54; N, 9.70%. FT-IR (diamond; cm^{-1}): 2959, 1598, 1436, 1356, 1212, 1056, 839, 743.

C15 In a manner similar to that described for **C1**, **C15** was prepared as a yellow powder in 89% yield. Anal. Calcd for $C_{21}H_{21}Cl_2N_3Ni$ (445.01): C, 56.68; H, 4.76; N, 9.44%. Found: C, 56.55; H, 4.87; N, 9.35%. FT-IR (diamond; cm^{-1}): 3351, 1592, 1527, 1458, 1353, 1129, 841, 775, 741.

C16 In a manner similar to that described for **C1**, **C16** was prepared as a yellow powder in 87% yield. Anal. Calcd for $C_{22}H_{23}Cl_2N_3Ni$ (459.04): C, 57.56; H, 5.05; N, 9.15%. Found: C, 57.43; H, 5.14; N, 9.10%. FT-IR (diamond; cm^{-1}): 2992, 1590, 1530, 1454, 1353, 1119, 842, 770, 731.

4.3. *General procedure for ethylene oligomerization*

Ethylene oligomerization under 10 bar ethylene was carried out in a stainless steel autoclave (0.25 L capacity) equipped with a mechanical stirrer, temperature controller, and gas ballast through a solenoid clave for the continuous feeding of ethylene at a constant pressure. The catalyst precursor was dissolved in 50 mL toluene in a Schlenk tube stirred with a magnetic stirrer and was injected into the reactor under an ethylene flux. The co-catalyst $EtAlCl_2$ and 50 mL toluene were added. When the required reaction temperature was reached, ethylene was introduced at the desired pressure to begin the reaction. After the reaction mixture was stirred for the desired period of time, the reaction was stopped and about 1 mL of the reaction solution was collected, and the reaction was terminated by the addition of 10% aqueous hydrogen chloride. The organic layer was analyzed by gas chromatography (GC) to determine the composition and mass distribution of the obtained oligomers.

4.4. *General procedure for norbornene polymerization*

Typically, 2.5 μmol of the nickel complex was dissolved in a Schlenk tube with 15.0 mL distilled toluene under nitrogen, and 14.3 mL of norbornene in toluene (3.50 M, 50.0 mmol of norbornene) was added via syringe. The polymerization was initiated by adding 1.72 mL

Table 5. Crystal data and structure refinement for **C2**·CH_3CH_2OH.

Crystal color	Yellow
Empirical formula	$C_{19}H_{18}Cl_2N_3NiO$
fw	433.97
T (K)	293(2)
Wavelength (Å)	0.71073
Crystal system	Triclinic
Space group	P1
a (Å)	9.2114(18)
b (Å)	9.801(2)
c (Å)	14.085(3)
α (°)	75.91(3)
β (°)	89.89(3)
γ (°)	82.04(3)
V (Å^3)	1220.8(4)
Z	2
D_{Calcd} (mg m^{-3})	1.181
μ (mm^{-1})	1.023
F(0 0 0)	446
Cryst. size (mm)	0.09 × 0.08 × 0.07
θ range (°)	1.49–27.48
Limiting indices	$-11 \le h \le 11$ $-12 \le k \le 12$ $-18 \le l \le 17$
No. of rflns. collected	13,450
No. unique rflns. [R(int)]	5409(0.0359)
Completeness to θ (%)	96.7
Abs. corr.	None
Data/restraints/parameters	5409/0/236
Goodness-of-fit on F^2	1.064
Final R indices [$I > 2\sigma(I)$]	$R1 = 0.0698$ $wR2 = 0.1914$
R indices (all data)	$R1 = 0.0742$ $wR2 = 0.1953$
Largest diff. peak and hole (e Å^{-3})	0.629 and −0.891

of toluene containing 1.46 mol L^{-1} MAO (2.5 mmol). After 20 min, the polymerization was terminated by injecting 200 mL of acidic ethanol (ethanol : HCl (conc.) = 95 : 5) into the reactor. Polynorbornene was isolated by filtration, washed with ethanol, and dried under vacuum at 60 °C for 12 h.

4.5. *Crystal structure determinations*

Single crystals of **C2**·CH_3CH_2OH, suitable for X-ray diffraction studies, were obtained by slow diffusion of diethyl ether into methanolic solution. Diffraction data for **C2**·CH_3CH_2OH were collected on a Rigaku Saturn724+ CCD with graphite-monochromated Mo-Kα radiation ($l = 0.71073$ Å). Cell parameters were obtained by the global refinement of the positions of all the collected reflections. Intensities were corrected for Lorentz and polarization effects in addition to empirical absorption. Data were collected using phi scans and the structures were solved by direct methods (SIR97) using SHELX97 [61], and the refinement was carried out by full-matrix least squares on F^2. All non-hydrogen atoms were refined anisotropically. Crystal data and processing parameters for **C2**·CH_3CH_2OH are summarized in table 5.

Supplementary material

CCDC 981264 contain the supplementary crystallographic data for the complexes **C2**·CH_3CH_2OH. These data can be obtained free of charge via http://www.ccdc.cam.ac.uk/conts/retrieving.html, or from the Cambridge Crystallographic Data Center, 12 Union Road, Cambridge CB2 1EZ, UK; Fax: (+44) 1223-336-033; or E-mail: deposit@ccdc.cam.ac.uk. Supplementary data associated with this article can be found in the online version.

Disclosure statement

No potential conflict of interest was reported by the authors.

Funding

This work was supported by National Natural Science Foundation of China [grant number 51474061]; Natural Science Foundation of Hebei Province [grant number B2014501120], [grant number E2013501035], [grant number E2013501135]; Program for New Century Excellent Talents in University [grant number NCET-10-0304]; Special Fund for Basic Scientific Research of Central Colleges, Northeastern University [grant number N100123003], [grant number N120523001]; Fund for the Scientific Research of Northeastern University at Qinhuangdao [grant number XNK201506]; State Key Laboratory of Chemical Resource Engineering, Beijing University of Chemical Technology.

References

[1] J. Skupinska. *Chem. Rev.*, **91**, 613 (1991).
[2] S. Mecking. *Coord. Chem. Rev.*, **203**, 325 (2000).
[3] W. Keim, F.H. Kowaldt, R. Goddard, C. Krüger. *Angew. Chem. Int. Ed. Engl.*, **17**, 466 (1978).
[4] W. Keim, A. Behr, B. Limbäcker, C. Krüger. *Angew. Chem. Int. Ed. Engl.*, **22**, 503 (1983).
[5] L.K. Johnson, C.M. Killian, M. Brookhart. *J. Am. Chem. Soc.*, **117**, 6414 (1995).
[6] L.K. Johnson, S. Mecking, M. Brookhart. *J. Am. Chem. Soc.*, **118**, 267 (1996).

[7] C.M. Killian, D.J. Tempel, L.K. Johnson, M. Brookhart. *J. Am. Chem. Soc.*, **118**, 11664 (1996).
[8] C.M. Killian, L.K. Johnson, M. Brookhart. *Organometallics*, **16**, 2005 (1997).
[9] S.A. Svejda, M. Brookhart. *Organometallics*, **18**, 65 (1999).
[10] B.Y. Lee, X. Bu, G.C. Bazan. *Organometallics*, **20**, 5425 (2001).
[11] V.C. Gibson, C.M. Halliwell, N.J. Long, P.J. Oxford, A.M. Smith, A.J.P. White, D.J. Williams. *Dalton Trans.*, **5**, 918 (2003).
[12] J.M. Benito, E. de Jesús, F.J. de la Mata, J.C. Flores, R. Gómez, P. Gómez-Sal. *Organometallics*, **25**, 3876 (2006).
[13] J.D. Azoulay, Y. Schneider, G.B. Galland, G.C. Bazan. *Chem. Commun.*, **41**, 6177 (2009).
[14] D.H. Camacho, Z. Guan. *Chem. Commun.*, **46**, 7879 (2010).
[15] H. Liu, W. Zhao, X. Hao, C. Redshaw, W. Huang, W.-H. Sun. *Organometallics*, **30**, 2418 (2011).
[16] R. Gao, K. Wang, Y. Li, F. Wang, W.-H. Sun, C. Redshaw, M. Bochmann. *J. Mol. Catal. A: Chem.*, **309**, 166 (2009).
[17] J. Yu, Y. Zeng, W. Huang, X. Hao, W.-H. Sun. *Dalton Trans.*, **40**, 8436 (2011).
[18] L. Zhang, X. Hao, W.-H. Sun, C. Redshaw. *ACS Catal.*, **1**, 1213 (2011).
[19] X. Hou, Z. Cai, X. Chen, L. Wang, C. Redshaw, W.-H. Sun. *Dalton Trans.*, **41**, 1617 (2011).
[20] T.R. Younkin, E.F. Connor, J.I. Henderson, S.K. Friedrich, R.H. Grubbs, D.A. Bansleben. *Science*, **287**, 460 (2000).
[21] T. Hu, L.-M. Tang, X.-F. Li, Y.-S. Li, N.-H. Hu. *Organometallics*, **24**, 2628 (2005).
[22] Q.-Z. Yang, A. Kermagoret, M. Agostinho, O. Siri, P. Braunstein. *Organometallics*, **25**, 5518 (2006).
[23] Q. Shi, S. Zhang, F. Chang, P. Hao, W.-H. Sun. *C.R. Chim.*, 10, 1200 (2007).
[24] M. Delferro, J.P. Mclnnis, T.J. Marks. *Organometallics*, **29**, 5040 (2010).
[25] D. Song, Y. Wang, H. Mu, B. Li, Y.-S. Li. *Organometallics*, **30**, 925 (2011).
[26] F. Speiser, P. Braunstein, L. Saussine, R. Welter. *Organometallics*, **23**, 2613 (2004).
[27] F. Speiser, P. Braunstein, L. Saussine. *Organometallics*, **23**, 2625 (2004).
[28] Z. Weng, S. Teo, T.S.A. Hor. *Organometallics*, **25**, 4878 (2006).
[29] P.W. Dyer, J. Fawcett, M.J. Hanton. *Organometallics*, **27**, 5082 (2008).
[30] W. Liu, J.M. Malinoski, M. Brookhart. *Organometallics*, **21**, 2836 (2002).
[31] P. Kuhn, D. Sémeril, D. Matt, M.J. Chetcuti, P. Lutz. *Dalton Trans.*, **5**, 515 (2007).
[32] N.A. Cooley, S.M. Green, D.F. Wass. *Organometallics*, **20**, 4769 (2001).
[33] Z. Guan, W.J. Marshall. *Organometallics*, **21**, 3580 (2002).
[34] F.A. Kunrath, R.F. de Souza, O.L. Casagrande Jr., N.R. Brooks, V.G. Young Jr.. *Organometallics*, **22**, 4739 (2003).
[35] N. Ajellal, M.C.A. Kuhn, A.D.G. Boff, M. Hörner, C.M. Thomas, J.-F. Carpentier, O.L. Casagrande Jr.. *Organometallics*, **25**, 1213 (2006).
[36] P. Hao, S. Zhang, W.-H. Sun, Q. Shi, S. Adewuyi, X. Lu, P. Li. *Organometallics*, **26**, 2439 (2007).
[37] W.-H. Sun, K. Wang, K. Wedeking, D. Zhang, S. Zhang, J. Cai, Y. Li. *Organometallics*, **26**, 4781 (2007).
[38] R. Gao, M. Zhang, T. Liang, F. Wang, W.-H. Sun. *Organometallics*, **27**, 5641 (2008).
[39] Q. Khamker, Y.D.M. Champouret, K. Singh, G.A. Solan. *Dalton Trans.*, **41**, 8935, (2009).
[40] J. Lai, X. Hou, Y. Liu, C. Redshaw, W.-H. Sun. *J. Organomet. Chem.*, **702**, 52 (2012).
[41] Y. Yang, P. Yang, C. Zhang, G. Li, X.-J. Yang, B. Wu, C. Janiak. *J. Mol. Catal. A: Chem.*, **296**, 9 (2008).
[42] H. Liu, L. Zhang, L. Chen, C. Redshaw, Y. Li, W.-H. Sun. *Dalton Trans.*, **40**, 2614 (2011).
[43] W. Zhang, Y. Wang, J. Yu, C. Redshaw, X. Hao, W.-H. Sun. *Dalton Trans.*, **40**, 12856 (2011).
[44] J. Hou, W.-H. Sun, S. Zhang, H. Ma, Y. Deng, X. Lu. *Organometallics*, **25**, 236 (2006).
[45] F.-B. Han, Y.-L. Zhang, X.-L. Sun, B.-G. Li, Y.-H. Guo, Y. Tang. *Organometallics*, **27**, 1924 (2008).
[46] F. Speiser, P. Braunstein, L. Saussine. *Dalton Trans.*, **10**, 1539 (2004).
[47] A. Kermagoret, F. Tomicki, P. Braunstein. *Dalton Trans.*, **22**, 2945 (2008).
[48] S.D. Ittel, L.K. Johnson, M. Brookhart. *Chem. Rev.*, **100**, 1169 (2000).
[49] V.C. Gibson, S.K. Spitzmesser. *Chem. Rev.*, **103**, 283 (2003).
[50] F. Speiser, P. Braunstein, L. Saussine. *Acc. Chem. Res.*, **38**, 784 (2005).
[51] V.C. Gibson, C. Redshaw, G.A. Solan. *Chem. Rev.*, **107**, 1745 (2007).
[52] C. Bianchini, G. Giambastiani, L. Luconi, A. Meli. *Coord. Chem. Rev.*, **254**, 431 (2010).
[53] C. Janiak. *Coord. Chem. Rev.*, **250**, 66 (2006).
[54] W.-H. Sun, H. Yang, Z. Li, Y. Li. *Organometallics*, **22**, 3678 (2003).
[55] B.Y. Lee, Y.H. Kim, H.J. Shin, C.H. Lee. *Organometallics*, **21**, 3481 (2002).
[56] A.A. Antonov, N.V. Semikolenova, V.A. Zakharov, W. Zhang, Y. Wang, W.-H. Sun, E.P. Talsi, K.P. Bryliakov. *Organometallics*, **31**, 1143 (2012).
[57] F. Blank, C. Janiak. *Coord. Chem. Rev.*, **253**, 827 (2009).
[58] T. Xiao, P. Hao, G. Kehr, X. Hao, G. Erker, W.-H. Sun. *Organometallics*, **30**, 4847 (2011).
[59] T. Xiao, S. Zhang, G. Kehr, X. Hao, G. Erker, W.-H. Sun. *Organometallics*, **30**, 3658 (2011).
[60] H.H. Nayeri, F.A. Taromi, M. Hemmati, F. Rekabdar. *J. Coord. Chem.*, **67**, 3270 (2014).
[61] G.M. Sheldrick. *SHELXTL-97, Program for the Refinement of Crystal Structures*, University of Göttingen, Germany (1997).